doi: 10.15407/ujpe61.03.0248

M.G. NAKHODKIN, M.I. FEDORCHENKO
Taras Shevchenko National University of Kyiv
(64/13, Volodymyrs'ka Str., Kyiv 01601, Ukraine)

PACS 73.20.At, 73.30.+y

PHOTOELECTRON EMISSION FROM Si–Gd–O CATHODE

Electronic and emission properties of photocathodes fabricated on the basis of multilayered structures of oxidized Gd atoms deposited on the Si(100) surface and additionally covered with fresh layers of Gd atoms have been studied as functions of the structure holding time under vacuum, by using the methods of photoelectron ($h\nu = 1.9 \div 10.2$ eV) and Auger electron spectroscopies. It is found that, although the photocathode work function is equal to about 0.5 eV at some research stages, the photoemission is registered only at $h\nu \geq 2.8$ eV. The analysis of the results allowed us to propose a model for the energy structure of the photocathode that agrees with experimental data. According to this model, the near-surface region of a photocathode, about 1 nm in thickness, consists of Gd_2O_3 with the energy gap width of about 5.3 eV. The distance from the Fermi level to the conduction band bottom equals about 2.7 eV in the Gd_2O_3 bulk. In the forbidden gap below the Fermi level, the bulk states and filled surface states associated with structural defects. A complicated dipole layer appears on the surface, and this gives the substantial reduction of the work function.

Keywords: adsorption, Gd, O, Si(100), oxidation, Gd_2O_3, work function.

1. Introduction

Researches of the interaction between rare-earth elements and the semiconductor surface are stimulated by both a possibility to practically use those systems and the necessity to improve the fundamental knowledge on the systems that contain elements with unfilled f shells [1–5]. In our previous works [6–8], we studied the interaction cycles of Gd and oxygen atoms with the Si(113) and Si(100) surfaces. It was found that, by creating a multilayered structure of oxidized Gd atoms, a photocathode with a low work function ($\varphi \approx 1$ eV) can be obtained. In work [8], we also found that the deposition of additional layers of Gd atoms on the surface of this photocathode changed its electronic and emission properties. Those properties also changed in time, as the photocathode is held in vacuum. In particular, the photocathode work function φ diminished to a value of about 0.5 eV. However, no detailed research of this phenomenon was carried out, and no energy structure for the photocathode was proposed.

This work continues the researches of the electronic and emission properties of photocathodes fabricated on the basis of a multilayered structure of oxidized Gd atoms deposited on the Si(100) substrate with the subsequent additional deposition of a layer of Gd atoms, exposure to oxygen, and holding in vacuum for some time. The aim of the work was to create a model for the electronic structure of this photocathode. Moreover, in order to obtain new features in the energy structure of the photocathode, we extended the spectral range of quanta used to excite photoelectrons.

2. Experimental Technique

The researches were carried out in a vacuum chamber with a basic pressure of about 1×10^{10} Torr. Like the previous works [6–8], we used low-energy electron diffraction (LEED), Auger electron spectroscopy, and photoelectron spectroscopy of the valence band with exciting photon energies $h\nu = 7.7$ and 10.2 eV. The required photons were generated with the aid of a discharge in hydrogen and a Seya–Namioka vacuum ultraviolet monochromator [9]. According to estimations made in work [10], the quantum flux intensity for the applied intense lines of a hydrogen discharge amounted to about 10^{10} quantum/s. In this work, we also used laser diodes as a source of photons with quantum energies of about 1.9, 2.3, 2.8, and 3.1 eV. On the basis of the power (10–100 mW) consumed by those sources, the intensity of a quantum

flux produced by them was estimated to lie within the approximate limits from 10^{16} to 10^{17} quantum/s.

The energy distributions of photoelectrons (the photoelectron spectra, PESs) were determined with the use of a spherical analyzer of the retarding type. Its spherical surface was covered with tin dioxide, which is characterized by a stable work function φ. The PESs were presented with respect to the Fermi level E_{F}. For quantum energies of 10.2 and 7.7 eV, the retarding potential U_{F}, which corresponded to E_{F}, was determined experimentally from PESs obtained for metal emitters with a considerable density of states at E_{F}. Among laser light sources, it was almost impossible to find a metal photocathode with a stable φ that would be lower than the energy of quanta emitted by lasers. Therefore, the magnitude of U_{F} that corresponded to E_{F} in the PESs excited with the use of laser sources was calculated, by assuming that a reduction in the light quantum energy by ΔE is accompanied by a reduction in the energy of electrons emitted from the level E_{F} by the same value, ΔE.

The research technique and the fabrication procedure of experimental specimens were described in our previous works [6–8]. The photocathode photosensitivity S in various photocathode states and its variations at various quantum energies $h\nu$ were determined from the changes of areas under the corresponding PES curves registered at constant quantum flux values. We did not determine the absolute values of quantum fluxes for every light source. Therefore, the presented data allowed the relative variations of S for quanta with a definite energy to be estimated only qualitatively.

Taking into account that the intensities of laser sources were 10^6–10^7 times higher than the intensities of sources with a monochromator, we had to check, first of all, whether the cathode properties did not change under the influence of such intense photon sources. For this purpose, PESs excited by only 10.2-eV (or 7.7-eV) photons and by the simultaneous action of 10.2-eV (or 7.7-eV) quanta and quanta with lower energies obtained from laser sources were measured. In Fig. 1, an example of such PESs for a typical Si–Gd–O photocathode is shown. The abscissa axis does not correspond to the difference $E - E_{\mathrm{F}}$, but to the bremstrahlung potential of the spectrum analyzer, U_R, in order to present PESs excited by the simultaneous action of quanta of two types with

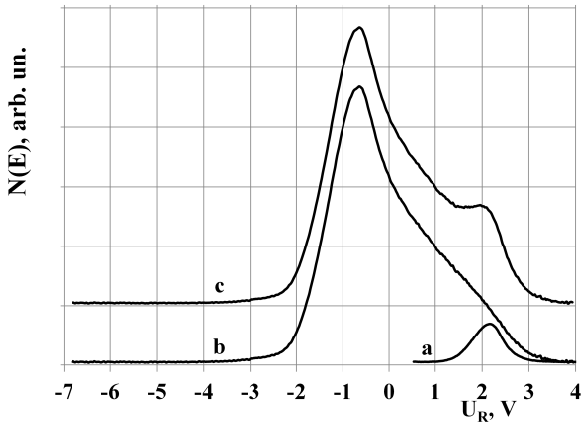

Fig. 1. PESs for a typical photocathode excited in various regimes: $h\nu = 3.1$ eV (a), $h\nu = 10.2$ eV (b), and $h\nu = 10.2$ and 3.1 eV (c) simultaneously

various energies. The same dependences were also obtained for $h\nu = 7.7$ eV, but they are not exhibited, because they do not differ qualitatively from the depicted ones. All those dependences testify that the PES excited by quanta with $h\nu = 3.1$ eV coincides with the differential PES between the spectra excited using the simultaneous action of quanta with various energies (10.2 and 3.1 eV) and only the action of quanta with an energy of 10.2 eV. The additive character of the PESs concerned means that no substantial modifications in photocathode properties take place under the action of powerful light sources with lower quantum energies.

The photocathode with φ close to 1 eV was used as an initial specimen. It was fabricated by applying a number of technological cycles consisting of the following stages: deposition of Gd atoms onto the Si(100) surface, adsorption of atomic oxygen, and annealing at $T \approx 600$°C. The routine was described in detail in our previous work [8]. The obtained photocathode turned out rather stable, keeping its properties constant even after plenty of test cycles. If necessary, the properties could be restored by annealing the photocathode at 600 °C.

3. Research Results

In Fig. 2, typical PESs of the photocathode measured within one of the testing cycles are depicted for $h\nu = 10.2$ (panel A) and 7.7 eV (panel B). Each of the testing cycles consisted of the following stages: stage b was the stage of the photocathode as an ini-

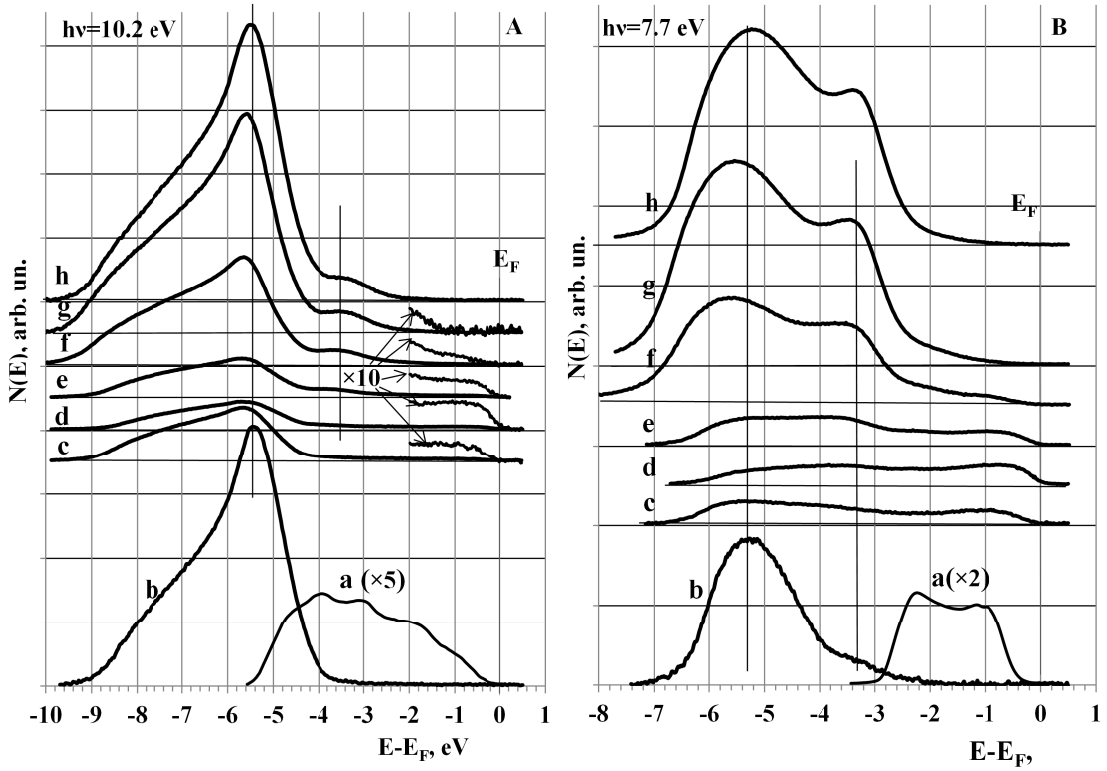

Fig. 2. PESs obtained at $h\nu = 10.2$ (A) and 7.7 eV (B) for the photocathode at various test stages within the same research cycle: atomically pure Si(100)-2×1 surface (a); typical initial specimen (b); after depositing Gd to a coverage of about 0.5 ML (c); after depositing Gd to a coverage of about 1 ML (d); after the holding of the system with the Gd coverage of about 1 ML in vacuum for 1, 3, 6, and 12 days, respectively (e)–(h)

tial specimen; at stages c and d, one monolayer (ML) of Gd was deposited onto the photocathode surface; and stages e to h were stages when the specimen was held in vacuum for various times. For the sake of comparison, curves a in Fig. 2 demonstrate PESs for the clean Si(100) surface of the substrate. One can see that the PESs of photocathode essentially differ from those of the substrate: the former reveal a maximum at the energy $E - E_{\rm F} \approx -5.4$ eV (i.e. 5.4 eV below $E_{\rm F}$). Like other authors did for similar systems [11–16], we attribute this maximum to the electron states O2p in gadolinium oxide. In addition, on the basis of Auger electron spectra (AESs), which are identical to those presented in our work [8] for a similar system, we come to a conclusion that Si atoms and SiO_2 molecules are practically absent in the near-surface layers of the examined photocathode. In the interval from 0 to 6 eV below $E_{\rm F}$, the presented PESs coincide with the PESs for Gd_2O_3, which were measured in work [16]. Therefore, we consider the near-surface region in our photocathode to consist mainly of gadolinium oxide. It is known from the literature that Gd_2O_3 has the energy gap width $E_g \approx 5.3$ eV [17–21]. All that allows us to suppose that the major contribution to the photoelectron emission belongs to the electrons excited from the valence band into the conduction band of the near-surface Gd_2O_3 layer. The thickness of this layer can be approximately evaluated to equal 1 nm, if the electron escape depth at $h\nu = 10.2$ eV [21] is used for this purpose. At a photon energy of 7.7 eV, the PESs of the initial specimen (Fig. 2B, curve b) contains a maximum at about 5.2 eV below $E_{\rm F}$ and a group of photoelectrons with a spectral peculiarity at an energy of about 3.2 eV below $E_{\rm F}$. It is evident [22] that the photoelectron escape depth at $h\nu = 7.7$ eV is larger than that at $h\nu = 10.2$ eV. Therefore, we may consider that the photoelectrons escape from larger depths at $h\nu = 7.7$ eV. As a result, they are scattered

more intensively before the escaping into vacuum, and their PES becomes more symmetric. We may assume that (i) the peak in the density of states, which is located by about 5.2 eV below E_F, is related to the electrons excited from the O2p states of gadolinium oxide and the scattered electrons excited from the valence band of the Si substrate; and (ii) the spectral peculiarity in the PESs at about 3.2 eV below E_F corresponds to the photoelectrons excited from the intermediate layer between Si and Gd_2O_3 or even from the Si substrate itself.

At stages c and d, when the Gd_2O_3 layer was additionally covered with Gd atoms – first to the coverage $\Theta_{Gd} \approx 0.5$ ML (stage c) and afterwards again to $\Theta_{Gd} \approx 0.5$ ML (stage d) – the PESs transform again (curves c and d in Fig. 2). (i) There appears a peak in the electron density of states at E_F (5d6s states of Gd atoms), which characterizes the appearance of a metal film on the photocathode surface. (ii) The intensity of PES peculiarities in the range from 5.2 to 5.4 eV below E_F decreases. (iii) The low-energy edge of PESs comes closer to E_F, which is associated with the growth of φ. In addition, the results of our researches carried out in this work and in work [8] testify to the appearance of the pure-Si LVV line and the non-oxidized-Gd NVV line in the AES of the specimen covered with a layer of oxidized Gd, when additional Gd layers are deposited on the latter. This fact allows us to assume that the deposition of additional Gd layers gives rise to the appearance of structural defects near the surface and localized electron states in the Gd_2O_3 energy gap, which are associated with those defects.

When the obtained system is held in vacuum, its PESs gradually change (Fig. 2, curves c to h). The spectral peculiarity associated with 5d6s states of Gd atoms near E_F decreases and almost disappears. The intensity of PES peculiarity in the interval from 5.2 to 5.4 eV below E_F grows. For $h\nu = 10.2$ eV (Fig. 2A), a PES peculiarity located in the interval from 3.3 to 3.4 eV below E_F appears and increases; for $h\nu = 7.7$ eV (Fig. 1B), this peculiarity increases more pronouncedly. The low-energy edge of PES curves shifts away from E_F, which is associated with a reduction of φ. After the specimen has been held in vacuum for 4 to 5 days, the value of φ decreased to about 0.5 eV. The variations in the PES and AES occur simultaneously. The Gd NVV line changes its shape, which takes place at the Gd oxidation. All the described variations in the PESs and AESs can be associated with the gradual oxidation of the film of Gd atoms, which was deposited on the photocathode surface, during the stay of the system in vacuum. Oxidation can take place owing to oxygen from the already existing Gd_2O_3 layer and from residual gases under the ultrahigh vacuum conditions. The exposure of the system in molecular oxygen to 50 L (1 L = 10^{-6} Torr s) accelerated the oxidation of the additional Gd layer, whereas an increase in the residual gas pressure in a vacuum chamber by two orders of magnitude for several hours practically did not affect the modification rate of surface electronic properties. This fact brings us to a conclusion that the oxidation of Gd atoms at the stages, where the photocathode is in vacuum, occurs with the aid of oxygen from the Gd_2O_3 layer.

It is reasonable to assume that the low value of φ for the Si surface subjected to the action of Gd and O atoms is a result of the formation of complicated dipole layers Gd–O–Gd and the formation of a surface with a negative electron affinity. However, special experiments showed that even if the formed surface had $\varphi \approx 0.5$ eV, its illumination with red ($h\nu \approx 1.9$ eV) or green ($h\nu \approx 2.3$ eV) laser quanta, the flux of which ($\approx 10^{16}$ quantum/s) was much more intense than the flux of 7.7-eV or 10.2-eV photons ($\approx 10^{10}$ quantum/s), did not stimulate the photoelectron emission. The photoeffect appeared only if a laser with a quantum energy of about 2.8 eV was used. This fact may mean that, on the way of the electron excitation into the conduction band, there is an energy barrier in the near-surface region. The barrier height is larger than the energy of green laser quanta ($h\nu \approx 2.3$ eV), but lower than the energy of blue laser quanta ($h\nu \approx 2.8$ eV). Unfortunately, we did not determine the barrier height more exactly for the lack of intense light sources with quantum energies between 2.4 and 2.8 eV. It is quite reasonable that the role of a barrier could play the energy gap in Gd_2O_3 and a barrier at the Si/Gd_2O_3 heterojunction. While carrying out experiments with slightly doped Si of the n-type (10 Ω cm) and heavily doped Si of the p-type (0.02 Ω cm), one may expect the formation of barriers with different heights at the Si/Gd_2O_3 heterojunction. The difference between the barrier heights should have been larger than at least half the energy gap in Si (0.56 eV). But the experiments showed that no changes in the conditions

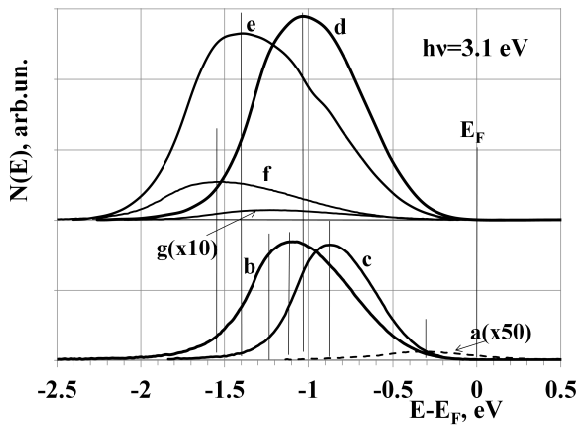

Fig. 3. PESs obtained at $h\nu = 3.1$ eV (B) for the photocathode at various test stages within the same research cycle: initial specimen (a); after depositing Gd to a coverage of about 0.5 ML (b); after depositing Gd to a coverage of about 1 ML (c); after holding the system with the Gd coverage of about 1 ML in vacuum for 1, 3, 6, and 12 days, respectively (d)–(g)

for the photoeffect to appear were observed. That is why we supposed that the photoemission barrier is somehow related to the energy gap width in Gd_2O_3.

In Fig. 3, typical PESs for the initial photocathode specimen, which were measured at $h\nu \approx 3.1$ eV in the same cycle of researches as was done at higher $h\nu = 7.7$ and 10.2 eV (see Fig. 2), are shown. The PESs in Fig. 3 are similar to Gaussian curves. Their maximum position and extent depend on the stage of a photocathode surface treatment. The maximum in the PES of the initial photocathode is observed at $|E - E_F| \approx 0.3$ eV (curve a). The deposition of additional Gd atomic layers within the coverage interval of 0.5–1.0 ML changes the intensity of the maximum and its position with respect to E_F (curves b and c). The spectrum extent, which is determined by the position of the low-energy PES edge relatively to E_F, i.e. by φ, also changes. The position of the PES maximum with respect to E_F, the maximum intensity, and the spectrum extent first increase and, having passed through a maximum, start to decrease. This means that, at those stages, there is a correlation between the position and the intensity of the PES maximum, area S under the PES curves, and work function, which can be observed at stages 0 to 2 in Fig. 5. At the next stages of the photocathode testing, when the photocathode is held in vacuum, the PES maxima first grow and shift together with the low-energy PES edges toward larger $|E - E_F|$ (curves d, e, and f). As the photocathode residence time in the vacuum increases, they start to decrease and shift in the opposite direction (curves f and g), which can be observed in Fig. 5 (stages 2 to 10), where the corresponding dependences of S and φ on the photocathode test stage number are depicted. At stages 2 to 4 and 7 to 10, there is a correlation between S and φ, whereas, at stages 4 to 6, it is absent. This circumstance and the presence of a maximum in the dependence of S on the stage number (Fig. 5) allow us to assert that two competing mechanisms dominate and govern the whole processes. First, this is a reduction of the work function, which increases the probability for the slowest photoelectrons to escape. Second, this is the oxidation of Gd atoms in the near-surface layer of the cathode, which diminishes the number of surface and localized states in the Gd_2O_3 energy gap in the near-surface photocathode region.

It should be noted that the oxidized layer of additionally deposited Gd atoms, which reduces the surface φ to about 0.5 eV, is weakly bound. After the cathode annealing to $T \approx 600$ °C, this layer becomes desorbed, and the surface restores its properties to the state of the initial photocathode. It is not ruled out that the annealing also reduces stresses and the concentration of defects near the surface.

4. Discussion of Results

In order to analyze the experimental data, a model for the electron structure in the formed photocathode is proposed (Fig. 4). This model is similar to those used for the explanation of the photoemission from photoemitters with a wide energy gap [23]. According to this model, the near-surface layer about 1 nm in depth in the initial photocathode specimen presumably consists of gadolinium oxide Gd_2O_3. This layer is created by subjecting the atomically pure Si(100) surface to a number of treatment stages. Each stage includes the deposition of Gd and O atoms followed by the annealing under ultrahigh vacuum conditions.

The energy gap width in Gd_2O_3 approximately equals 5.3 eV [17–21]. The distance E_F to the bottom of the conduction band in the Gd_2O_3 bulk is accepted to equal 2.7 eV, because even in the case where the work function for the photocathode $\varphi \approx 0.5$ eV, the photoelectrons are excited only by quanta with $h\nu \geq 2.8$ eV. In the energy gap below E_F, the bulk states and filled surface states associated with struc-

tural defects are localized. The band bending downward near the surface does not exceed 0.1 eV, because, while forming this structure, no appreciable change in the positions of photoelectron spectra features with respect to E_F was detected at a reduction of φ.

A complicated dipole layer responsible for a reduction of φ is formed at the surface. The distance from E_F to the vacuum level E_{vac} on the surface equals about 1.2 eV. Hence, we obtain a surface with the negative electron affinity $\chi \approx -1.5$ eV. The model also predicts the excitation of slow photoelectrons (<2 eV) and photoelectrons with higher kinetic energies. Low-energy quanta ($h\nu = 2.8 \div 3.1$ eV) excite low-energy photoelectrons from defect states in the energy gap, whereas quanta with higher energies ($h\nu = 7.7$ and 10.2 eV) excite photoelectrons in a wider energy range. Some of the latter electrons can be scattered at their motion toward the surface, so that they lose their initial energy.

Let us apply this model and qualitatively consider the behavior of photocathode during a typical cycle of researches, which consists of the stages described in the previous section. In Fig. 5, the dependences of the work function φ and the photosensitivity S on the treatment stage number within the same cycle of researches are plotted for two quantum energies: 3.1 and 10.2 eV. The corresponding data were calculated from the dependences shown in Figs. 2 and 3. The results obtained for $h\nu = 7.7$ eV are not shown, because they are qualitatively similar to those for $h\nu = 10.2$ eV.

First of all, we attract attention to that the values of S which are formed by slow photoelectrons at $h\nu \approx 3.1$ eV are several orders of magnitude lower than the S-values, which are mainly formed by photoelectrons with higher kinetic energies ($E - E_F \approx \approx -5.3$ eV) at $h\nu = 10.2$ eV. This fact is typical of the comparison of the impurity and intrinsic photoeffects. Again, the S-values obtained at high and low energies of quanta correlate in different manners with the change of φ. For photoelectrons excited by quanta with energies of 7.7 and 10.2 eV, the S-values completely correlate with the change of φ in a wide interval of this parameter. As φ grows, the S-values decrease, and *vice versa*. In the case of slower photoelectrons excited by quanta with lower energies, the S-values both increase and decrease when φ diminishes. It is so, because the parameter S for slow photoelectrons depends not only on φ, but also on

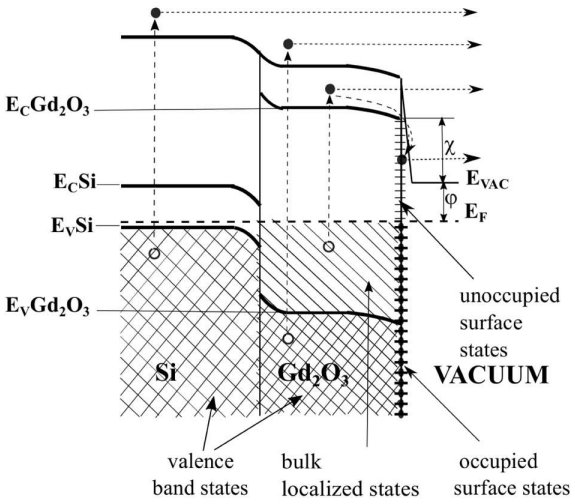

Fig. 4. Energy diagram of the system Si-Gd_2O_3

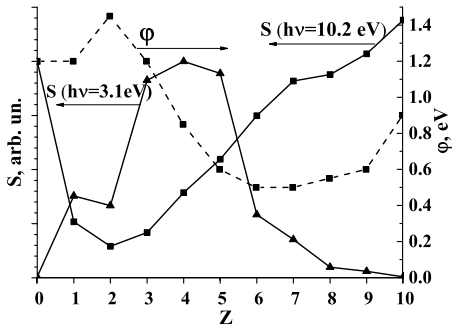

Fig. 5. Typical dependences of S and φ on the stage number in the same research cycle obtained at $h\nu = 10.2$ and 3.1 eV: $Z = 0$ corresponds to the initial specimen (*1*); deposition of 0.5-ML Gd coverage, deposition of 1-ML Gd coverage (*2*); holding of the cathode in vacuum for 1, 2, 3, 5, 6, 7, 9, and 12 days, respectively, *3–10*. S was normalized by S_0 for $h\nu = 10.2$ eV, and by S_{max} for $h\nu = 3.1$ eV

the change in the number of local defect and impurity levels in the near-surface layer of photocathode, when Gd is deposited and the system is held in vacuum.

Hence, the energy model proposed for our photocathode does not contradict the photocathode properties known at present. It can be used while planning further researches of this system. For the model to be tested and further improved, it is necessary that researches of the optical properties and the structural homogeneity of photocathode should be carried out.

5. Conclusions

Using the electron spectroscopy methods, the electronic and emission properties of a photocathode with a low work function ($\varphi \approx 1.2$ eV) fabricated on the basis of a multilayered structure of oxidized Gd atoms (Gd_2O_3) deposited onto a Si(100) surface have been studied. The application of photons with low (1.9 eV $< h\nu <$ 3.07 eV) and high (7.7 eV $<$ $< h\nu <$ 10.2 eV) energies in the researches of the photocathode photosensitivity and PESs allowed two groups of photoelectrons to be distinguished in the spectra. One group includes photoelectrons excited by low-energy photons from local electron states and filled surface states in the energy gap of Gd_2O_3. The other group includes photoelectrons excited by high-energy photons from the states in the valence band of Gd_2O_3. The analysis of the results and the literature data allowed us to propose a model for a possible energy structure of the photocathode. The model agrees with experimental data and can be used for planning new researches, as well as for further improvement of our knowledge concerning such systems.

1. H.D.B. Gottlob, A. Stefani, and M. Schmidt, J. Vac. Sci. Technol. B **27**, 258 (2009).
2. J.H.G. Owen, K. Miki, and D.R. Bowler, J. Mater. Sci. **41**, 4568 (2006).
3. D. Lee, D.K. Lim, S.S. Bae, S. Kim, R. Ragan, D.A. Ohlberg, Y. Chen, and R.S. Williams, Appl. Phys. A **80**, 1311, (2005).
4. H. Zhanq, Q. Zhanq, G. Zhao, J. Tang, O. Zhou, and L.C. Qin, J. Am. Chem. Soc. **127**, 13120 (2005).
5. Byung-Chun, R. Motohash, C. Lorder, and R. Jansen, Nature Mater. **5**, 817 (2006).
6. M.G. Nakhodkin and M.I. Fedorchenko, Visn. Kyiv. Univ. Ser. Fiz. Mat. Nauky **4**, 261 (2012).
7. M.G. Nakhodkin and M.I. Fedorchenko, Visn. Kyiv. Univ. Ser. Fiz. Mat. Nauky **1**, 239 (2014).
8. M.G. Nakhodkin and M.I. Fedorchenko, Ukr. J. Phys. **60**, 97 (2015).
9. M.E. Akopyan, I.I. Balyakin, and F.I. Vilesov, Prib. Tekhn. Eksp. N 6, 96 (1961).
10. V.K. Adamchuk, Ph.D. thesis (Leningrad State Univ., Leningrad, 1969) (in Russian).
11. K. Wandelt and C.R. Brundle, Surf. Sci. **157**, 162 (1985).
12. G. Molnar, G. Peto, and E. Kotai, Vacuum **41**, 1640 (1990).
13. W.A. Henle, M.G. Ramsey, F.P. Netzer, R. Cimino, S. Witzel, and W. Braun, Surf. Sci. **243**, 141 (1991).
14. J.C. Chen, G.H. Shen, and L.J. Chen, Appl. Surf. Sci. **142**, 291 (1999).
15. Ya.B. Losovyj, D. Wooten, J.C. Santana, J.M. An, K.D. Belashchenko, N. Lozova, J. Petrosky, A. Sokolov, J. Tang, W. Wang, N. Arulsamyand, and P.A. Dowben, J. Phys.: Condens. Matter. **21**, 045602 (2009).
16. C.R. Abernathy, A.H. Gila, and A.H. Onstine, J. Semicond. Sci. Technol. **3**, No. 1, 13 (2003).
17. *Materials and Reliability Handbook for Semiconductor Optical and Electronic Devices*, edited by O. Ueda and S.J. Pearton (Springer, New York, 2013).
18. S.S. Derbeneva and S.S. Batsanov, Dokl. AN SSSR **175**, 1062 (1967).
19. S.S. Batsanov and E.V. Dulepov, Sov. Phys. Solid State **4**, 995 (1965).
20. K.A. Gschneidner, *Rare-Earth Alloys* (Van Nostrand, Princeton, 1961).
21. Jun-Kyu Yang and Hunng-Ho Park, Appl. Phys. Lett. **87**, 022104 (2005).
22. I. Lindau and W.E. Spicer, J. Electron Spectrosc. Relat. Phenom. **3**, 409 (1974).
23. A.A. Pakhnevich, V.V. Bakin, A.V. Yazykov *et al.*, Pis'ma Zh. Eksp. Teor. Fiz. **79**, 592 (2004).

Received 22.01.09.
Translated from Ukrainian by O.I. Voitenko

М.Г. Находкін, М.І. Федорченко

ФОТОЕЛЕКТРОННА ЕМІСІЯ КАТОДА Si–Gd–O

Р е з ю м е

Методами фотоелектронної ($h\nu$ = 1,9—10,2 еВ) та ожеелектронної спектроскопій досліджено зміни електронних та емісійних властивостей фотокатода на основі багатошарової структури окислених атомів Gd на підкладці із Si(100) після напилення на його поверхню додаткових шарів атомів Gd та з часом перебування цієї структури в вакуумі. Було встановлено, що незважаючи на те, що робота виходу фотокатода на окремих етапах досліджень становила ≈0,5 еВ, фотоемісія реєструвалась лише для $h\nu \geq$ 2,8 еВ. Аналіз отриманих результатів досліджень дозволив запропонувати модель імовірної енергетичної структури фотокатода, яка узгоджується з експериментальними даними. У відповідності з цією моделлю приповерхнева область фотокатода складається із Gd_2O_3 товщиною ≈1 нм і шириною забороненої зони ≈5,3 еВ. Відстань від рівня Фермі до дна зони провідності в об'ємній частині Gd_2O_3 дорівнює ≈2,7 еВ. В забороненій зоні нижче рівня Фермі розташовані об'ємні локалізовані стани та заповнені поверхневі стани, зумовлені дефектами структури. На поверхні утворюється складний дипольний шар, відповідальний за зменшення роботи виходу.